

Interfaces between phases in a lattice model of microemulsions

K. A. Dawson*

*Department of Chemistry, Cornell University, Baker Laboratory, Ithaca, New York 14853-1301
and Laboratory of Atomic and Solid State Physics, Cornell University, Ithaca, New York 14853-2501*

(Received 15 August 1986)

A lattice model which has recently been developed to aid the study of microemulsions is briefly reviewed. The local-density mean-field equations are presented and the interfacial profiles and surface tensions are computed using a variational method. These density profiles describing the interface between oil rich and water rich phases, both of which are isotropic, are structured and non-monotonic. Some comments about a perturbation expansion which confirms these conclusions are made. It is possible to compute the surface tension to high numerical accuracy using the variational procedure. This permits discussion of the question of wetting of the oil-water interface by a microemulsion phase. The interfacial tensions along the oil-water-microemulsion coexistence line are ultra-low. The oil-water interface is not wet by microemulsion throughout most of the bicontinuous regime.

I. INTRODUCTION

Recently Widom has described a lattice model of microemulsions. The reader who is interested in details should consult the original paper.¹ The purpose of the present article is limited to discussing the behavior of surfactant molecules near interfaces within the context of the lattice model. Later papers will deal with global aspects of the phase diagram, critical points, critical end points, and considerations beyond the mean-field theory, so no attempt will be made to report these results in this account.

The origins of the lattice model may be understood in the following way. The three components, oil, water, and amphiphile, are conceived to have only two types of functional group. Hydrophilic (water-like) and hydrophobic (oil-like) residues are labeled *A* and *B*, respectively. The three species may then be named *A-A*, *A-B*, *B-B* according to their functionality.

In calculating the partition function for this system, one should count all possible configurations of these molecules. However, it is clear that contributions where *A* and *B* ends of different molecules are close together are quite small. Now imagine dividing configuration space into cubes of side *a*. We make the following approximation. Only arrangements where each cube is filled with either all *A* or *B* ends are permitted. Furthermore, the interactions are viewed as constant inside each cube and it is now possible to assign a density of *A* or *B* heads to each such portion of space. A lattice with vertices lying at the centers of the cubes defines the lattice gas ($\rho_n = 1, 0$) or equivalent spin model ($\sigma_n = \pm 1$) in the following sense. If a cube is filled with *A* or *B* heads, then the spin variable is set to +1 or -1. When the various interaction terms are included and the partition function calculated, it is possible to show that the model is equivalent to an Ising system with one-spin, nearest-neighbor (NN), next-nearest-neighbor (NNN)—linear and diagonal—and three-spin couplings. The coupling constants are *H*, *J*,

M, *2M*, and *L*, respectively. A transcription of these to solution variables is given in Table I. Note that for $l = h = 0$ (the symmetrical regime) there are equal amounts of oil and water in the mixture. This is expected to correspond to part of the bicontinuous region of the microemulsion phase diagram. Most of the following remarks refer to this two-parameter cut of the phase diagram.

It is now possible to construct a mean-field theory of this model based on the local density of *A* heads (ρ_n) at each lattice site $\mathbf{n} = (x, y, z)$. The spin variables are related to site density by $\rho_n = \frac{1}{2}(S_n + 1)$ where $S_n = \langle \sigma_n \rangle_0$. The notation $\langle x \rangle_0$ means that the average of *x* is calculated using the mean-field Hamiltonian. The mean-field equations for $l = h = 0$ are

$$[-m \Delta_n^4 - (j + 12m) \Delta_n^2 - 6(j + 5m)] S_n + \tanh^{-1} S_n = 0, \tag{1.1}$$

TABLE I. Translation of Ising spin to microemulsion variables.

$$\zeta = \left(\frac{Z_{BB}}{Z_{AA}} \right)^{1/2}, \quad \xi = \left(\frac{Z_{AB}}{(Z_{AA} Z_{AB})^{1/2}} \right)^{1/2}.$$

Z_{ij} is the activity of *ij* species, $q = K/kT$, $j = J/k\theta$, $h = H/k\theta$, $m = M/k\theta$, $l = L/k\theta$. The energies of interaction of two *A* or *B* ends of different amphiphiles are $K(1-\lambda)$ and $K(1+\lambda)$. The temperatures of the solution and Ising models are *T* and θ , respectively.

Ising model	Microemulsion model
<i>j</i>	$-\ln \xi + (5/2)q$
<i>h</i>	$3 \ln \zeta + (15/4)\lambda q$
<i>m</i>	$-\frac{1}{4}q$
<i>l</i>	$-\frac{1}{4}\lambda q$

where Δ_n^2 is the three-dimensional lattice difference operator and $\Delta_n^4 = (\Delta_n^2)^2$. For certain portions of the (j, m) plane the symmetry of solutions is planar and Eqs. (1.1) become [see Figs. 1(a) and 1(b)]

$$[-m\Delta_z^4 - (j + 12m)\Delta_z^2 - 6(j + 5m)]M_z + \tanh^{-1}M_z = 0, \quad (1.2)$$

which are equivalent to those of the axial NNN Ising (ANNNI) model.^{1,2} The general theory will be developed elsewhere. However, if we confine ourselves to the region where $-m/(j + 8m) > 0$, $1/(j + 3m) > 0$, the phase dia-

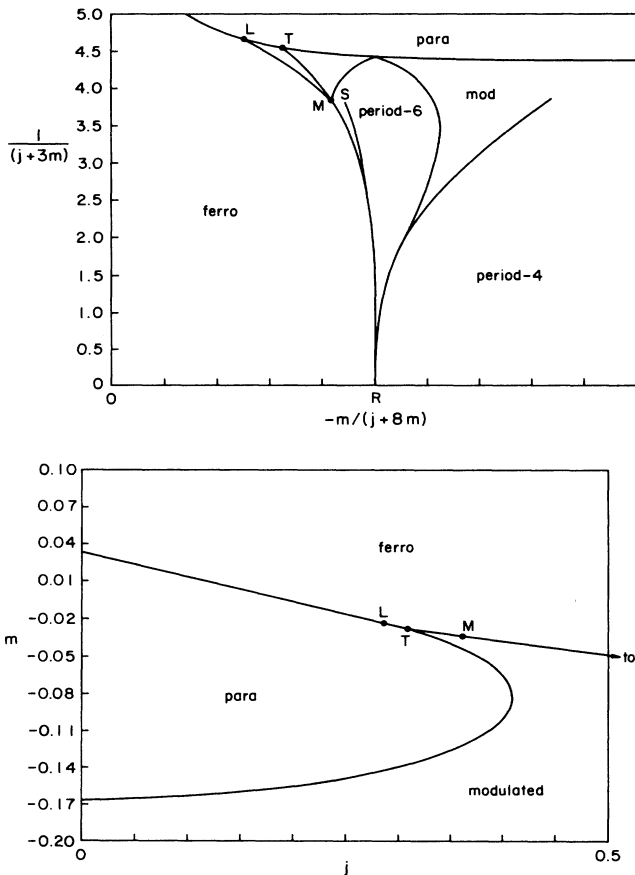


FIG. 1. (a) The phase diagram for part of the symmetrical ($l, h = 0$) lattice model. The plot is in conventional axial NNN Ising (ANNNI) model variables [$1/(j + 3m)$ vs $-m/(j + 8m)$]. Only the important phase boundaries are drawn. The curve RT is the three-phase ($\alpha:\gamma$:period-6) coexistence line. Along MT it is the metastable extension of RM . The curve ML is the three-phase ($\alpha:\gamma$:modulated phases) coexistence line where all three phases are global minima of the free energy. The curve RS is the locus where $\sigma_{\alpha\gamma} = \sigma(0)$ is zero. To the left of it $\sigma_{\alpha\gamma}$ is positive. (b) The half-plane ($j > 0$) phase diagram for the symmetrical ($l, h = 0$) lattice model. In this case m has been plotted against j . Only those phase boundaries relevant to the surface tension calculations are drawn. The phase diagram for $j < 0$ may be constructed from the positive half-plane by a simple symmetry operation.

grams of the two models are the same. The ferromagnetic ($+, -$) phases occupy a two-phase region bounded largely by a second-order line (to the paramagnetic phase) and a first-order line dividing it from a modulated phase of period six ($\langle 3 \rangle$ phase in the notation of Ref. 2). In solution language the ferromagnetic phases are bulk oil or water, with some surfactant solubilizing the other material. The modulated phase is one where there are three consecutive layers (comprised of basic cubes) largely filled with A heads, and then three with B heads. The surfactant molecules are mostly confined to the regions where layers of oil and water meet.

The remainder of this paper is divided into three sections. In Sec. II we examine the interfacial structure and tension between the oil rich and water rich phases. In Sec. III we give an analytical description of these interfaces. In Sec. IV we discuss the problem of wetting of the oil-water interface by the microemulsion phase. Results are sometimes presented in terms of the traditional ANNNI model variables J_0, J_1, J_2 [$J_0/kT = j + 3m$ and $-J_2/J_1 = -m/(j + 8m)$]. This should facilitate comparisons with the results of those who have studied the anisotropic magnetic model.

II. INTERFACIAL STRUCTURE AND TENSION

Equations (1.2) will first be written in terms of ρ_z , the density of A ends at lattice plane z . Remember that, strictly speaking, the density within each cube is constant and given by the density at lattice index n . The lattice plane z is formed by the centers of an infinite two-dimensional array of cubes with equal density. Thus, we seek density profiles $\{\rho_z\}$ which minimize the free energy ($M_z = 2\rho_z - 1$),

$$F = \sum_z [-3(j + 5m)(2\rho_z - 1)^2 - (j + 12m)(2\rho_z - 1)\Delta_z^2\rho_z - m(2\rho_z - 1)\Delta_z^4\rho_z + \rho_z \ln \rho_z + (1 - \rho_z) \ln(1 - \rho_z)], \quad (2.1)$$

and satisfy boundary conditions $\rho_z \sim \rho_\infty$ as $z \rightarrow \infty$ and $\rho_z \sim (1 - \rho_\infty)$ as $z \rightarrow -\infty$, corresponding to bulk oil rich and water rich phases. The numerical results (examples of which are presented in Figs. 2–5) are essentially exact within mean-field theory. This was achieved by using each ρ_z as an independent variational parameter and increasing the length (in the direction of z) until there was no change in the free energy per spin, typically $O(10^{-10}kT)$. Initial studies also addressed the question of avoiding metastable profiles connecting ρ_∞ and $(1 - \rho_\infty)$. This was done in a number of ways (including a “heat bath” technique) but experience and the analysis of Sec. III soon permitted the confident choice of initial conditions. One of the most striking features of the density profiles is that they are no longer monotonic (except for the case of $m = 0$ which corresponds to the nearest-neighbor Ising model). Although a simple analysis (see Sec. III) shows that this must be so, the physical origins of the effect are a little more subtle. By examining the distribution of surfactant molecules across the interfacial

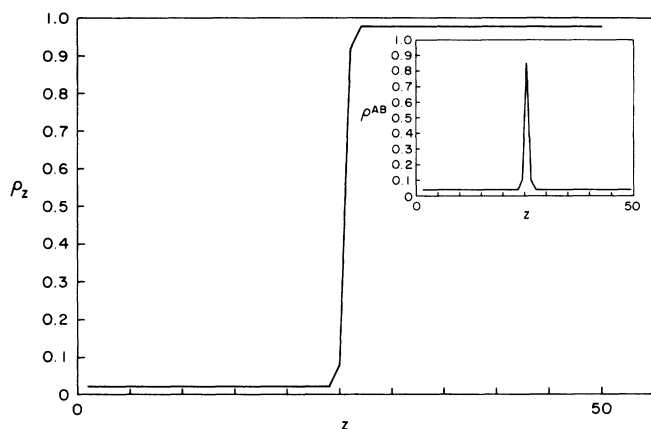


FIG. 2. Density of A functions at lattice plane z for three sets of parameter values. These are $1/(j+3m)=3.844$ and $-m/(j+8m)=0.02$ (Fig. 2), 0.08 (Fig. 3), 0.48 (Fig. 4). They lie along a horizontal line in Fig. 1(a). The insets have been constructed using Eq. (A3) and represent the density of AB bonds across lattice planes z and $z+1$.

region, one can draw the following conclusions. Most surfactant molecules are found at the interface where they cause a great reduction of surface tension. Also, because of the tendency of hydrophobic groups to repel hydrophilic groups, amphiphiles tend to cause aggregation of material at either side of the interface. This results in structure in the interface to a distance of the bulk correlation length (ξ). Figure 6 shows that this is an important effect in the following sense. The surface tension is calculated by subtracting the bulk free energy from the free-energy when an interface is present. This latter contribution is computed by summing the free-energy density, an example of which is presented in Fig. 6. Notice that ultra-low surface tensions arise as a result of subtle free-energy can-

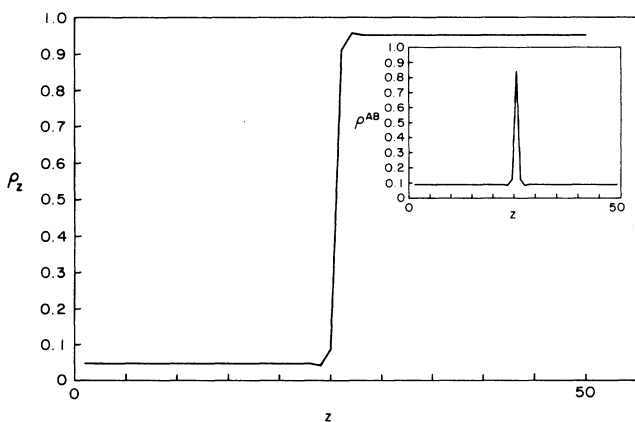


FIG. 3. Density of A functions at lattice plane z for three sets of parameter values. These are $1/(j+3m)=3.844$ and $-m/(j+8m)=0.02$ (Fig. 2), 0.08 (Fig. 3), 0.48 (Fig. 4). They lie along a horizontal line in Fig. 1(a). The insets have been constructed using Eq. (A3) and represent the density of AB bonds across lattice planes z and $z+1$.

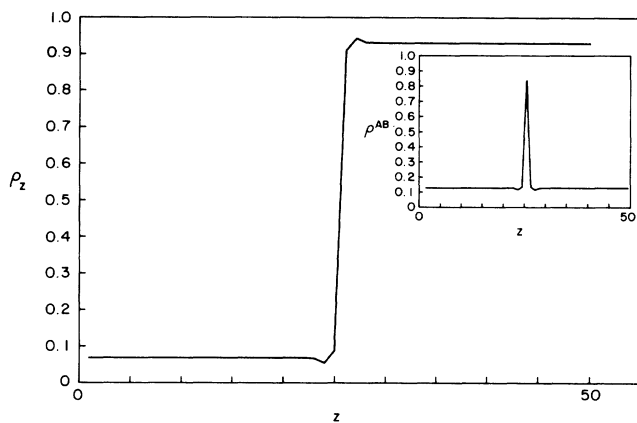


FIG. 4. Density of A functions at lattice plane z for three sets of parameter values. These are $1/(j+3m)=3.844$ and $-m/(j+8m)=0.02$ (Fig. 2), 0.08 (Fig. 3), 0.48 (Fig. 4). They lie along a horizontal line in Fig. 1(a). The insets have been constructed using Eq. (A3) and represent the density of AB bonds across lattice planes z and $z+1$.

cellations across the interface. In the context of the lattice model, this is a direct consequence of the interfacial density oscillations. Thus, a monolayer of surfactant is not in itself sufficient to ensure that the surface tensions found in this model are in agreement with those observed. If the model has captured the essential features of microemulsions and surfactant solutions, then one would expect, in experiments, to observe structure reminiscent of the nearest (metastable) bulk phase at the interface between homogeneous phases.

The qualitative features of the surface tension throughout the two-phase region are evident from Figs. 7 and 8. In every instance the surface tension is given in units of $k\theta/a^2$ unless otherwise stated. The quantitative results for $m=0$ agree with earlier calculations by Widom³ on the nearest-neighbor Ising model. In Fig. 8 we

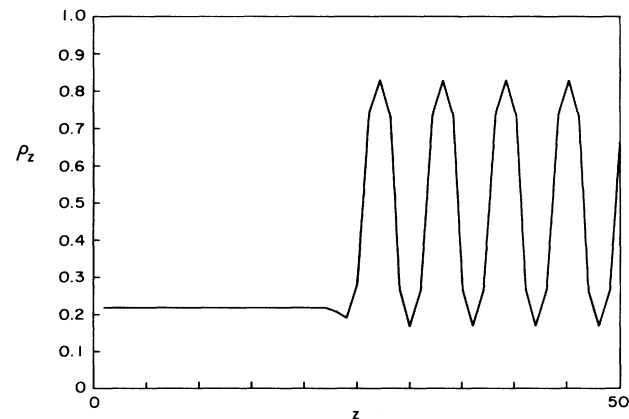


FIG. 5. Density of A functions at lattice plane z for the α - β (period-6) interface. This calculation is for a point on the three-phase coexistence line RM and just beneath M in Fig. 1(a).

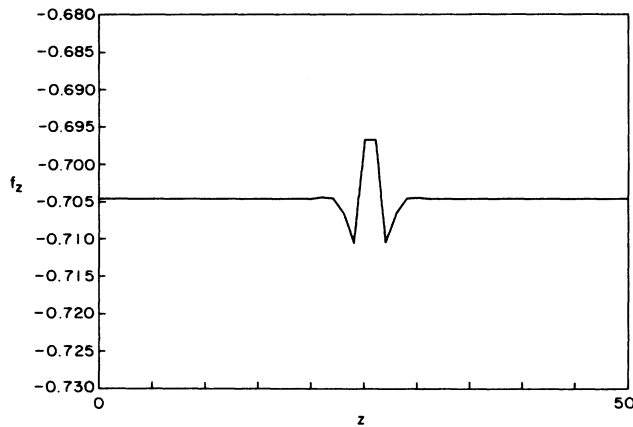


FIG. 6. Free-energy density at lattice plane z . The surface tension is obtained from the integral minus the bulk free energy.

show the surface tension plotted against $-m/(j+8m)$ for a number of different values of $1/(j+3m)$, i.e., along horizontal lines in Fig. 1(a). Note that results have been presented even for the region where bulk oil rich and water rich phases are metastable with respect to microemulsion. To the left of the line RS in Fig. 1(a) the surface tension is positive. This line is the locus of points where $\sigma=0$. To the right of it, the bulk states remain metastable minima, but this interfacial profile is no longer stable. Thus, the interface (in the absence of gravity) has infinite response to some long-wavelength transverse fluctuation: The interface would crumple. Note that at low (Ising) temperature the line of stability is close to the line $j+10m=0$. At zero temperature these two lines meet. Finally, it is clear that when the interface is unstable there are two possibilities: Either the system degenerates to the

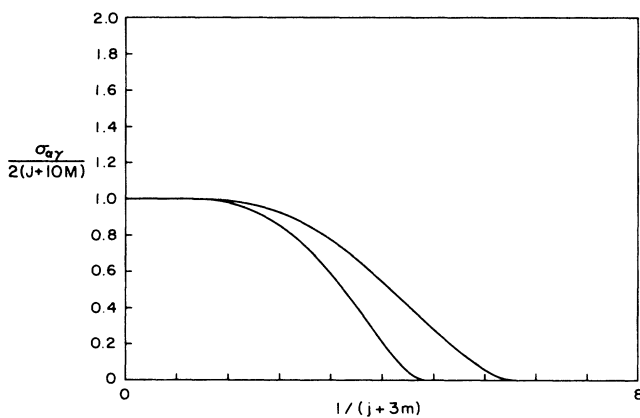


FIG. 7. Normalized surface tension $[\sigma/2(J+10M)]$ vs $1/(j+3m)$. Upper curve, simple Ising model ($m=0$); lower curve, $j+12m=0$. This latter set of parameter values corresponds to a vertical line [in Fig. 1(a)] which intersects the Lifshitz point L .

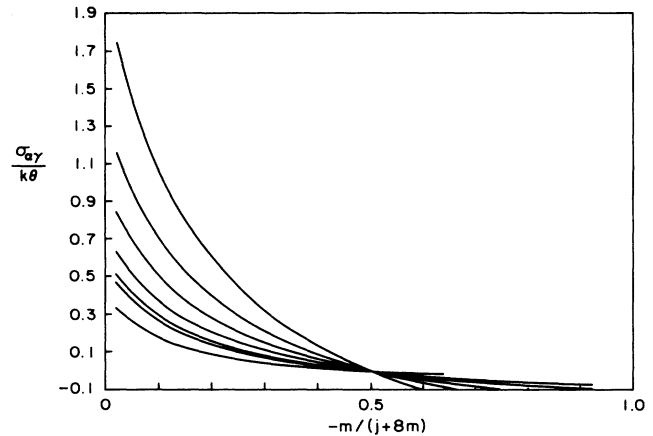


FIG. 8. Surface tension of α - γ interface (fixed $1/(j+3m)$) vs $-m/(j+8m)$. At $m=0$ the curves (from the top) correspond to $1/(j+3m)=1.0, 1.5, 2.0, 2.5, 2.844, 3.0, 3.5$. Note that the density-profile plots of Figs. 2–4 were calculated along the line $1/(j+3m)=2.844$.

modulated phase that is the global minimum, or it can find another local minimal free-energy interface which is stable with respect to transverse oscillations. This point will be elaborated elsewhere.

III. ANALYTICAL TREATMENT OF INTERFACES

The appearance of nonmonotonic density profiles due to surface aggregation may be a little surprising if one is accustomed to normal liquid-gas interfaces. It is thus worth providing some analytical insight into the novel features presented by a fourth-order gradient term. We present the following material in the spin representation for simplicity. One should bear in mind that the density of A heads in layer z is simply given by $\rho_z = \frac{1}{2}(M_z + 1)$, while the density of B heads is just $(1 - \rho_z)$.

As outlined below Eq. (2.1), we wish to solve the Euler equations subject to the conditions $M_z \sim \pm M_0$ which represent bulk oil- and water-phase asymptotes. However, both theoretical arguments and experience of computations such as those of Sec. II indicate that the interfacial region is only of dimension 2ξ , where ξ is the bulk correlation length. Furthermore, even within the interfacial region, the deviation of the density profile from the left or right asymptotes is fairly small. Thus, rather than expanding in temperature series we choose to use the bulk phase densities as the zeroth approximation in an iterative solution (rather like the Born series of scattering theory).

Imagine that the lattice planes are situated at half-odd integer values of z . To the right or left of the origin and beginning at $z = \frac{1}{2}$ or $-\frac{1}{2}$ we assign the density M_0 or $-M_0$ (see Fig. 4). The actual density profile deviates from $\pm M_0$ by the (small) value $\pm f_z$. The zeroth-order approximation to M_z of Eq. (1.2) then satisfies

$$6(j+5m)M_0 = \tanh^{-1} M_0. \quad (3.1)$$

The first-order correction then follows by linearizing around this uniform density. Thus

$$L_z f_z^{(1)} = [-m \Delta_z^4 - (j + 12m) \Delta_z^2] f_z^{(1)} - 6(j + 5m) + (1 - M_0^2)^{-1} f_z^{(1)} = 0. \quad (3.2)$$

The Green function of this operator may be defined in terms of the inverse susceptibility of the bulk phases with respect to small perturbations. Thus

$$G_{z,z'} = \frac{1}{2} \frac{\partial^2 F}{\partial M_z \partial M_{z'}} = L_z \delta_{z,z'}, \quad (3.3)$$

which may be diagonalized in a basis of plane waves. The Fourier transform $(-\pi, \pi)$ of the Green function is just the inverse (momentum-dependent) susceptibility,

$$\chi_q^{-1} = K_q^{M_0} = -4(j + 3m) + (1 - M_0^2)^{-1} - 2(j + 8m) \cos q - 2m \cos(2q). \quad (3.4)$$

The solutions of (3.2) correspond to plane waves with momenta $\pm q, \pm q^*$ such that χ_q diverges. The roots of (3.4) are

$$\cos q = -\frac{1}{4m}(j + 8m) \pm \frac{1}{8m} [4j^2 + 86m^2 + 16m(1 - M_0^2)^{-1}]^{1/2}, \quad (3.5)$$

providing m is nonzero. These roots are, in general, complex. If $q = \beta + i\alpha$, and (u, v) are the real and imaginary parts of the right-hand side of (3.5),

$$\begin{aligned} \cosh \alpha \cos \beta &= u, \\ \sinh \alpha \sin \beta &= v. \end{aligned} \quad (3.6)$$

To this order the density profile is given by

$$M_z \sim \begin{cases} M_0 - A e^{-\alpha z} \cos(\beta z + \phi), & z > 0 \\ -M_0 + A e^{\alpha z} \cos(\beta z + \phi), & z < 0 \end{cases}$$

where A and ϕ are undetermined. These constants are fixed by consideration of quadratic terms in (3.2).

This sort of expansion has limited use in discussing wetting and other delicate questions. However, it emphasizes the point that the qualitative features of the mean-field interfacial profile are determined by the four complex divergences of the susceptibility. Naturally, for the simple nearest-neighbor Ising model, one has $m = 0$ and (3.4) has only real roots. This is reflected in the monotonic density profile of Fig. 2.

IV. THE QUESTION OF WETTING

From the phase diagram it is clear that there is a three-phase coexistence line which becomes asymptotically close to $j + 10m = 0$. This is the locus (RT) where oil rich, water rich, and modulated ($\langle 3 \rangle$) phases have the same free energy, and each phase satisfies the Euler equations (1.2). These conditions have been used to locate the first-order line to high numerical accuracy.

It is now of interest to compare the surface tensions between oil rich and water rich phases ($\sigma_{\alpha\gamma}$) and either of

these with the microemulsion phase ($\sigma_{\alpha\beta} = \sigma_{\beta\gamma}$). When

$$\sigma_{\alpha\gamma} = \sigma_{\alpha\beta} + \sigma_{\beta\gamma}, \quad (4.1)$$

the contact angle⁴ becomes zero and the β phase is said to wet the $(\alpha:\gamma)$ interface.

This problem was investigated using mean-field theory in the following way. Imagine interposing l complete cycles of the period-6 phase between bulk α and γ phases. We label this configuration $(\alpha:\beta^l:\gamma)$ where $l=0$ corresponds to the normal $(\alpha:\gamma)$ interface. This choice is made because very unfavorable free energies result from using fractions of half cycles of the β phase. It is now possible to compute the surface tension $[\sigma(l)]$ as a function of l along the three-phase line. When the global minimum is $l=0$ or ∞ the $(\alpha:\gamma)$ interface is wholly nonwet or completely wet. In this instance the surface tension at fixed j and m increases monotonically with increasing l . Beyond $l=3$, $\sigma_{\alpha\gamma}(l)$ is essentially $2\sigma_{\alpha\beta}$. The relevant results of these calculations when β is the period-6 phase are presented in Figs. 9–11. The one-parameter family of $\sigma(l=0) = \sigma_{\alpha\gamma}$ along the three-phase coexistence line is plotted in Fig. 9. If $\sigma(l=1, 2, \dots, \infty)$ data were plotted on this graph, there would be no discernible deviation from the $\sigma_{\alpha\gamma}$ data. Hence in Fig. 10 an expanded scale plot of $\sigma_{\alpha\gamma}$ (symbols \bullet) and $2\sigma_{\alpha\beta}$ (symbols \circ) is presented. Since, in this instance, $\sigma_{\alpha\beta} = \sigma_{\beta\gamma}$, the crossing of these two line yields the wetting transition. Note carefully that this occurs in the part of the phase diagram where all of α, γ, β (period-6 phase) are metastable. The three-phase coexistence line is, at this point, the metastable extension of the three-phase line at lower temperature. Wetting would thus occur only if one could quench all three phases to the point $(W) j_w^{(3)} = 0.36347$ and $m_w^{(3)} = -0.03491$. The symbol $j_w^{(3)}$ denotes that value of the coupling parameter at which the $\langle 3 \rangle$ phase wets the $(\alpha:\gamma)$ interface. The point marked M ($j = 0.366$, $m = -0.035$) on Figs. 1(a) and 9 marks the upper limit where the three coexisting phases α, β (period 6), and γ

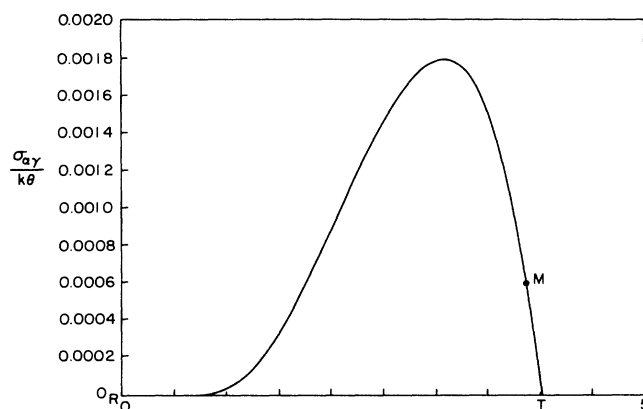


FIG. 9. Surface tension vs $1/(j+3m)$ along three-phase coexistence line RM . To the right of the point M (along MT), α, γ , and period-6 phases are in metastable coexistence. The wetting transition point (where the period-6 phase wets the interface between α and γ phases) is just beneath M (along MT).

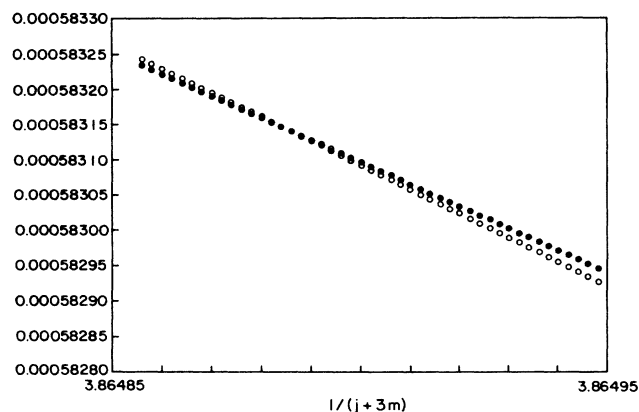


FIG. 10. Surface tensions of α - γ (symbol \bullet) and α - β (symbol \circ) interfaces vs $1/(j+3m)$. Wetting transition at intersection.

are global minima (but see Appendix B where the location of M is discussed). It is thus clear that along the line RM , the interface is never wet by the β (period-6) phase. One final check on this conclusion is possible. Thus at the values of the coupling constants $(j_w^{(3)}, m_w^{(3)})$ the period-7 ($\langle 34 \rangle$) phase is found to have a lower free energy than that of the period-6 phase. Clearly, then, the point M lies before the point W on the line RT .

There remains the following interesting but open question. Does one of the longer-period modulated phases (which replace the period-6 solution in the three-phase equilibrium along ML wet the $(\alpha:\gamma)$ interface? Until one has fully understood the phase diagram above the point M , it is not possible to resolve this question. For example, it has been suggested² that a branching process involving combinations of three and four consecutive spins occurs. Based on our investigations it seems likely that one of these modulated phases does eventually wet the oil-water interface. Also, in the conventional ANNNI model one has more freedom in coupling-parameter space (J_0, J_1, J_2 rather than j, m). It is thus probable that the (metastable)

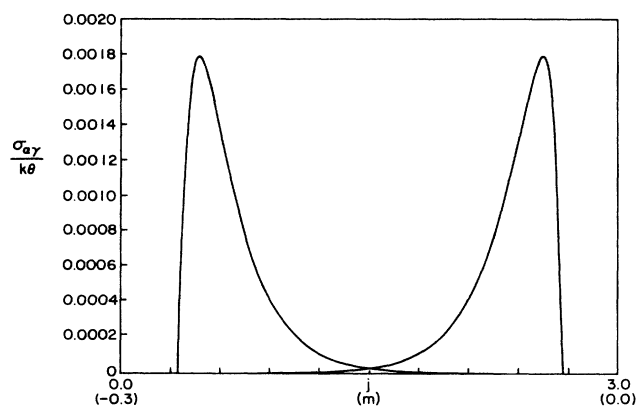


FIG. 11. Surface tension of α - γ interface along the three-phase line RT vs j (left) and m (right).

wetting transition by the $\langle 3 \rangle$ phase can be brought into the region where the three coexisting phases are global minima. The resolution of the question is probably not important to our understanding of the microemulsion model. At the point M the α and β (period-6) phases contain 33.5% and 37.6% of surfactant molecules. These concentrations are too large to be relevant to what are usually thought of as microemulsions.

Finally, note that at zero Ising (and solution) temperature $\sigma_{\alpha\gamma}$ and $2\sigma_{\alpha\beta}$ become equal. Although this is not really a wetting transition, the trend to smaller contact angles at low temperature might be reflected in experimental data.

V. CONCLUSIONS

The purpose of this research was to extend our understanding of the lattice model of microemulsions. The results of the study are encouraging. Thus, a model with prescribed microscopic interactions has been able to reproduce extremely low bulk interfacial tensions along the three-phase line. In fact [see comments beneath equation (A7)] even the quantitative results seem reasonable. In addition, it is predicted that the oil rich, water rich interface is not wet by microemulsion in the symmetrical region of the phase diagram. This is in accord with experimental surface tension data⁵ and direct visual observation.⁶ It is worth noting that a transition to wetting has been observed in some systems,⁷ but not in others.⁸ The transition, when it occurs, does so in the unsymmetrical regime (l, h nonzero in lattice model language). It will be interesting to compare the predictions of the lattice model with these results. Some of the detailed findings of this research [density profiles, the presence of the line RS in Fig. 1(a), etc.] are, at the moment, of more theoretical than experimental interest.

The results of more extensive studies of surface tension, critical points, and critical end points of the lattice model will be reported in the near future. Detailed phase diagrams (for two- and three-dimensional lattices) calculated by mean-field and simulation methods will also be published.

ACKNOWLEDGMENTS

The author thanks Doctor M. D. Lipkin and Professor B. Widom for many helpful discussions and comments while this work was in progress. He also acknowledges a useful conversation about the contents of Sec. IV with Professor M. E. Fisher and Ms. A. Liu. The research was supported in part by the Laboratory of Atomic and Solid State Physics (Cornell University) and the Lindemann Trust (through the English Speaking Union) which provided financial support. It is part of a program supported by the National Science Foundation and the Cornell University Materials Science Center.

APPENDIX A

In this appendix we discuss some of the details of the composition-profile and surface tension plots of Figs. 2–11. Recall that ρ_n and $(1-\rho_n)$ are the local densities of

A- and *B*-type functions within the cube surrounding lattice site \mathbf{n} . In the interfacial density plots we have plotted ρ_z against z . The points (ρ_z, z) have been joined by straight lines as a guide to the eye. However, one should keep in mind the fact that densities are constant within each cube of side a . Also, note that the free energy of the profile is invariant to translation by any integer.

To analyze the distribution of surfactant molecules, one uses the idea that the *A*—*B* “bonds” lie across neighboring cubes containing different head groups. It is then possible to write the density of bonds at $n + \frac{1}{2}\hat{\mathbf{t}}$ ($\hat{\mathbf{t}}$ is a unit vector in the direction $\hat{\mathbf{i}}, \hat{\mathbf{j}}$, or $\hat{\mathbf{k}}$) in terms of the correlation function,

$$\rho_{n+1/2}^{AB} = \frac{1}{2} \langle (1 - \sigma_n \sigma_{n+1}) \rangle, \quad (\text{A1})$$

where the subscripts “ $n + \frac{1}{2}$ ” and “ $n + 1$ ” are now shorthand for $n + \frac{1}{2}\hat{\mathbf{t}}$ and $n + \hat{\mathbf{t}}$. Within mean-field theory, spin-spin correlation functions factor. Thus

$$\rho_{n+1/2}^{AB} = -2\rho_n \rho_{n+1} + \rho_{n+1} + \rho_n. \quad (\text{A2})$$

Note that Eq. (A1) is an exact formula while (A2) is correct only with the mean-field approximation. Equation (A2) is the generalization of an approximate formula given by Widom.³ If one is studying layered states or planar interfacial profiles, Eq. (A2) becomes

$$\rho_{z+1/2}^{AB} = -2\rho_z \rho_{z+1} + \rho_{z+1} + \rho_z \quad (\text{A3})$$

and this result has been used to construct the insets to Figs. 2–4. Furthermore, by neglecting derivatives in a gradient expansion of (A3), one obtains Eq. (21) of Ref. 3.

It is also possible to calculate the fraction X_{AB} of surfactant molecules in any bulk state,

$$X_{AB} = \frac{1}{3N} \sum_{x,y,z} (\rho_{x+(1/2)yz}^{AB} + \rho_{xy+(1/2)z}^{AB} + \rho_{xyz+(1/2)}^{AB}), \quad (\text{A4})$$

for layered phases with period p (symbolized n , $n = p/2$) and modulation in the z direction,

$$X_{AB}^n = \frac{1}{3p} \sum_{z=1}^p (-4\rho_z^2 - 2\rho_{z+1}\rho_z + 5\rho_z + \rho_{z+1}). \quad (\text{A5})$$

If the period-6 state has site densities $X, Y, X, (1-X), (1-Y), (1-X)$ and the α, γ phases have density ρ_∞ and $(1-\rho_\infty)$, respectively,

$$X_{AB}^\infty = 2\rho_\infty(1-\rho_\infty), \quad (\text{A6})$$

$$X_{AB}^3 = \frac{1}{9}(-6X^2 + 8X - 4Y^2 + 6Y - 4XY + 1). \quad (\text{A7})$$

At zero Ising (and solution) temperature $\rho_\infty = 0$ and $X = Y = 0$. Hence, the fraction of surfactant molecules in the α or γ phase is zero, while the period-6 (microemulsion) phase is comprised of 11.1% surfactant, 44.45% oil, and 44.45% water. At the point $1/(j+3m) = 1.344$, $-m/(j+8m) = 0.499$, the $(\alpha:\gamma)$ surface tension is

typical of those observed experimentally [$\sigma_{\alpha\gamma} \sim 2 \times 10^{-4}(k\theta/a^2)$]. It is interesting to note that the associated proportions of *AB* molecules in the three phases (oil, water, microemulsion) are then 0.35%, 0.35%, and 11.3%.

Regarding the units used in plotting surface tensions, the following conventions were found to be convenient. For horizontal cuts in the phase diagram [Fig. 1(a)] it is possible to use $\sigma/k\theta$. For vertical cuts (Fig. 7) it is preferable to normalize to the zero-temperature surface tension. This is calculated by considering the energy of a profile $M_z = \pm 1(z \pm ve)$. Thus

$$\frac{\sigma_{\alpha\gamma}}{k\theta} \rightarrow 2(j+10m) \text{ as } \theta \rightarrow 0 \quad (\text{A8})$$

throughout the $\alpha:\gamma$ region. The $(\alpha:\gamma)$ surface tension vanishes in the limit $j+10m = 0$, $(j+3m) \sim \infty$. For higher (Ising) temperatures the locus of vanishing surface tension is plotted on Fig. 1(a). This is determined numerically from the data in Fig. 8.

APPENDIX B

As explained in Sec. IV, the location of the wetting transition for the period-6 phase is straightforward. However, in deciding where the three-phase line becomes metastable (M), one requires a few additional assumptions. These are based on an asymptotic expansion around the critical line (to be published) and appear to be reasonable. Thus one believes that the order of stability of the modulated phases near the paramagnetic, modulated-phase boundary is preserved along the line ML . It is then likely that the period-6 phase (in coexistence with α, γ phases) can become unstable only with respect to solutions of type $\langle 3^p 4^q \rangle$ (see Ref. 2). It is now possible to solve Eqs. (1.2) along the $(\alpha:\langle 3 \rangle:\gamma)$ line assuming these periodicities as initial conditions. When the free energy of one of these becomes lower than that of the $\langle 3 \rangle$ phase, one has approximated the point M . This procedure was carried out for small values of p and q . Among this trial set of solutions only those of the form $\langle 3^p 4 \rangle$ (of which the first is of period 7) have free energies that ever cross that of the α, γ , and $\langle 3 \rangle$ phases on the $(\alpha:\langle 3 \rangle:\gamma)$ line. The $p = \infty$ limit of these crossings occurs at $j = 0.366$, $m = -0.035$ [$1/(j+3m) = 3.844$, $-m/(j+8m) = 0.415$] while the $(\alpha:\langle 3 \rangle:\gamma)$ wetting transition is found to occur at $j_w = 0.36347$, $m_w = -0.03491$ [$1/(j+3m) = 3.86489$, $-m/(j+8m) = 0.41463$].

The vicinity of the point M is at present being studied (in association with P. Balbuena) using annealed Langevin minimizations. It will soon be possible to be more rigorous in the description of this point of the phase diagram. As outlined in Sec. IV, one cannot be definitive about wetting by longer-period modulated phases until this question is fully elucidated.

*Permanent address: Department of Physical Chemistry, The University of Leeds, Leeds, LS2 9JT, England, United Kingdom.

¹B. Widom, J. Chem. Phys. **84**, 6943 (1984); see also M. Schick and Wei-Heng Shih, Phys. Rev. B **34**, 1797 (1986).

²W. Selke and P. M. Duxbury, Z. Phys. B **57**, 49 (1986); M. E.

- Fisher and W. Selke, *Philos. Trans. R. Soc. London* **302**, 1 (1981).
- ³B. Widom, *J. Phys. Chem.* **88**, 6508 (1984).
- ⁴J. S. Rowlinson and B. Widom, *Molecular Theory of Capillarity* (Clarendon, Oxford, 1982).
- ⁵A. Pouchelon, J. Meunier, D. Langevin, D. Chatenay, and A. M. Cazabat, *Chem. Phys. Lett.* **76**, 277 (1980); A. M. Cazabat, D. Langevin, J. Meunier, and A. Pouchelon, *Adv. Colloid Interface Sci.* **16**, 175 (1982); A. M. Bellocq, D. Bourbon, B. Lemanceau, and G. Fourche, *J. Colloid Interface Sci.* **89**, 427 (1982).
- ⁶H. Kunieda and K. Shinoda, *Bull. Chem. Soc. Jpn.* **55**, 1777 (1982); K. Shinoda, *Prog. Colloid Polym. Sci.* **68**, 1 (1983); D. Chatenay, O. Abillon, J. Meunier, D. Langevin, and A. M. Cazabat, *Macro- and Microemulsions*, Vol. 272 of *ACS Symposium Series*, edited by Dinesh O. Shah (American Chemical Society, Washington, D.C., 1985).
- ⁷J. Meunier, *J. Phys. Lett.* (to be published).
- ⁸J. van Nieuwkoop and G. Snoei, Shell Research B. V., Report No. 674 (January 1983) (unpublished).